



Research Article

SIMULATION OF SHRINKAGE EFFECT IN DRYING OF FOOD PRODUCTS IN HOT-AIR DRYER

Burak TURKAN*¹, **Akin Burak ETEMOGLU**²

¹Bursa Uludag University, Mechanical Engineering Department, BURSA; ORCID: 0000-0002-4019-7835

²Bursa Uludag University, Mechanical Engineering Department, BURSA; ORCID: 0000-0001-8022-1185

Received: 07.08.2019 Revised: 02.01.2020 Accepted: 06.03.2020

ABSTRACT

Simulation of the hot-air drying period is very significant to decrease energy expenditure and increase food quality effect. In the present study, drying kinetics of three different foods (carrot, eggplant and cucumber) were investigated experimentally. At the end of the 180 minute drying process, the maximum change in moisture content was found to be in eggplant with 83%. The simulation model developed for hot-air drying was used to solve the heat and mass transfer equations which include shrinkage effect for food products. The shrinkage effect was obtained using the Arbitrary Lagrangian Eulerian method. At the end of the drying process, volume change for carrot, cucumber and eggplant were obtained as 55.7%, 55.7% and 68.7% respectively. On the other hand, the numerical model defines the internal moisture distributions of the food depending on the time. In this study, furthermore, empirical data were applied to different drying models. Statistical conclusions indicated that the Midilli model was the best to explain the drying behaviour for cucumber ($R^2=0.99$, $SEE=0.0077$, $x^2=6.00 \times 10^{-5}$) and eggplant ($R^2=0.99$, $SEE=0.0169$, $x^2=0.0003$). However, Wang and Singh model was found to be the most suitable model for carrot ($R^2=0.99$, $SEE=0.0054$, $x^2=2.95 \times 10^{-5}$). The experimental data were compared with numerical results for the drying of carrots, eggplant, and cucumber. It was shown a very good agreement between numerical simulation and experimental solution.

Keywords: Food drying, numerical and experimental investigation, shrinkage, thin drying models, hot-air drying.

1. INTRODUCTION

The carrot contains vitamins B1, B2, B6 and B12 is a rich nutritious food product. It also contains carotene and carotenoids. Carrot has a good taste and must be consumed fresh [1, 2]. The eggplant is grown in North America, Asia, and the Mediterranean region. It is important to keep the eggplant fresh for a long time in terms of shelf life. Drying is required to provide more stable food products and to ensure their use all year round [3]. Water that fruits and vegetables contain causes chemical degradation. Therefore, the drying process is used for the long-term conservation of agricultural products. With the drying process, the long-term healthy storage of seasonally produced foods is ensured without losing their vitamin value. Thus, the economic waste is prevented, and a long-term quality product is presented to the consumer [4]. Therefore, it is vital

* Corresponding Author: e-mail: burakt@uludag.edu.tr, tel: (224) 294 07 45

to minimize the moisture content. It is difficult to determine how much moisture remains at any point in the food during drying, experimentally. Therefore, the numerical analysis of the drying process is very important. By using the numerical method, the temperature and moisture distribution of the food can be easily estimated depending on the time. During the drying time, shrinkage is observed due to the evaporation of moisture from the product. The shrinkage effect occurring in food products has an observable strong impact on the structure of the dried food and the drying rate [5].

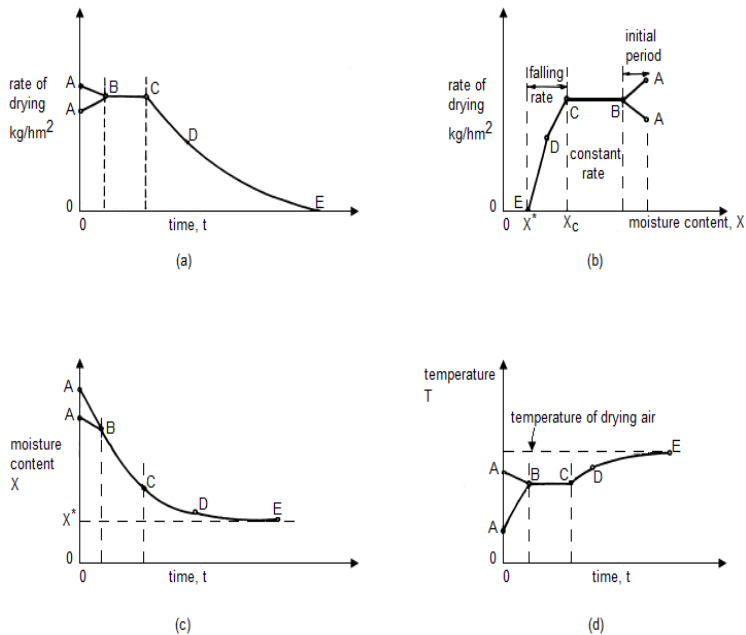


Figure 1. a) Change of drying rate over time b) Change of drying rate with moisture content c) Change of moisture content over time d) Change of temperature over time

In the drying process, hot air flow is sent over the material, which leads to heat convection and removes water from the food material. This process depends on the relative moisture and temperature of the air and continues until the moisture in the product reaches equilibrium. The mass of water, which transfers via evaporation as a function of the unit area and time, determines the drying rate. When a moist product, which has a surface covered with a water film, begins to dry, the drying rate is equal to the evaporation rate. The drying rate does not change as long as the air velocity, temperature and moisture remain constant. The moisture that starts to disappear from the water film on the surface is referred as the first critical moisture. The constant velocity period is called the ongoing drying period until the critical moisture is reached. The changing character of the drying process is described in terms of four experimentally determined graphs, as shown in Figure 1.

- AB : Process of heating or cooling moist product before equilibrium
- BC : The constant evaporation of liquid in constant-rate period
- C : The first critical point where dry spots begin to form on the surface of the moist product
- CD : First falling-rate period
- D : The second critical point where the surface is completely dry
- DE : Second falling-rate period

The moisture of the product continuously decreases over time in different periods. Because the external conditions (air velocity, moisture, and temperature) are constant, by controlling the drying air, the surface temperature is fixed in the range of BC to achieve uniform evaporation of liquid. The heat transfer is balanced by the mass transfer in the BC area.

In the constant-rate period, the surface temperature of the material is equal to the wet-bulb temperature of drying air. Then, the amount of moisture in the material begins to decrease due to increased resistance, i.e., the moisture transfer from the interior to the surface of the material becomes more difficult. The drying rate does not remain constant due to the ongoing drying process of the solid product, and the water film starts to disappear at the first critical moisture point C. After a while, the water film on the surface completely disappears. After this point, a continuous decrease in mass transfer is observed. This period is called the falling-rate period. Point D is the second critical moisture point. While the drying depends on the movement rate of the water through the material to the surface, the drying rate continues to decrease. The moisture in the product is reduced to equilibrium with the relative moisture of drying air. As a result of the drying of the surface of the product and the increase in the surface temperature during the falling rate period, structure and quality defects appeared in the product. Hygroscopic moisture loss occurs as a consequence of exceeding the critical moisture value. Thus, the drying process is preferred in BC area where the critical moisture value is not exceeded. The surface is completely dry at the second critical point. The heat that is transferred to the surface in falling rate period exceeds the energy required for evaporation. The surface temperature increases to the dry bulb temperature. As a result, mass transfer decreases, and moisture equilibrium is reached [6].

Fick's law of diffusion is used for defining the dehydration kinetics. The thin-layer drying models obtained by using this law are frequently encountered in the literature. The Lewis model [7], Henderson and Pabis model [8], Two Term model [9], Wang and Singh model [10], Midilli model [11] can be given as examples of these models.

Many studies on drying have been done in the literature. Vega et al. [12] investigated the maximum temperature value of the fruit and vegetables on the product surface. They dried the apple slices experimentally in the automatic control unit. In the simulation model, they defined the optimal control with experimental data. Bezerra et al. [13] calculated the moisture diffusivity and mass transfer coefficients using the analytical model in the literature for drying the food. Experimental and correlated results were obtained. Udayraj et al. [14] have developed a numerical model for estimating the moisture content of a food product. In the study of Kaya et al. [15] used a convective dryer to study the drying behavior of the cucurbit. Lemus-Mondaca et al. [16] studied the drying of a solid food product using different drying air temperatures from 40°C to 80°C both numerically and experimentally. Kumar et al. [17] developed a mathematical model of simultaneous heat and mass transfer during forced drying with forced convection. Darıcı and Sen [18] studied kiwi drying experimentally. In the literature, there are studies of drying of many different food products using convective drying method; okra [19]; prunes [20]; red pepper [21]; carrot [22]; peach [23]; tomatoes [24]; kiwi [25], apple [26].

In literature, drying kinetics of food products were significantly examined. However, it was not found that the shrinkage effect was examined by Arbitrary Lagrangian Eulerian method for different food products (carrot, cucumber and eggplant). In this study, it was aimed to obtain the drying features of carrot, cucumber, and eggplant. For this purpose, the characteristics were obtained experimentally, and the drying conditions were modeled and compared with the numerical study, including the shrinkage effect. Five drying models were used to provide the closest result of the experimental data. Finally, the compatibility of the results obtained with the drying models in the literature was investigated.

2. MATERIALS AND METHODS

Carrot, eggplant, and cucumber were used in the experiments. Drying processes were accomplished using a convective tunnel-type dryer (Ogen, Turkey). The experimental schematic diagram was presented in Figure 2.

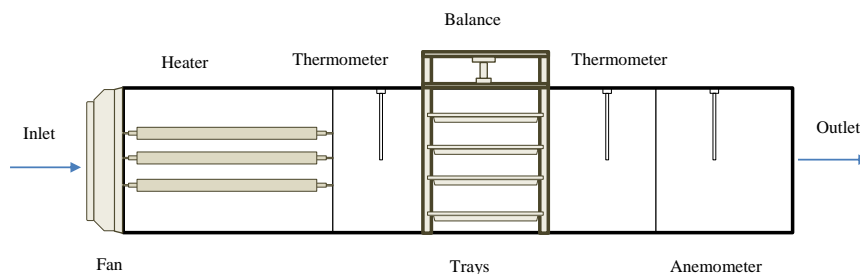


Figure 2. Experimental set up of tunnel type convective dryer

Carrot, eggplant, and cucumber slices weighing 93 ± 0.05 g were placed in a dryer to determine the initial moisture and dried at an air temperature of $60 \pm 0.3^\circ\text{C}$ for 24 hours. Drying was continued until the difference between the last two values fell below 1%. The average initial moisture content on a wet basis of the foodstuff (carrot, eggplant, and cucumber) was found to be 79.51%, 92.3%, and 88.56%, respectively. The air temperature of $60 \pm 0.3^\circ\text{C}$ and the air velocity of 0.7 m/s were used. Carrot, eggplant, and cucumber were sliced to 1 cm thickness and 2.5 cm in diameter. The change in the weight of the foods was registered with a digital scale (Kern, Germany) with a sensitivity of 0.05 g. Air velocity were measured in an anemometer (± 0.1), while air temperature measurement (± 0.3) was performed with a thermometer in the experimental set up. The food surface temperature was made non-contact with infrared temperature meter (TESTO 845) with $\pm 0.1^\circ\text{C}$ sensitivity.

2.1. Calculation of Moisture Content

Eq.1 and Eq.2 define dry and wet basis expressions as follows:

$$M_{DB} = \left(\frac{W_w}{W_{dr}} \right) = \left(\frac{W - W_{dr}}{W_{dr}} \right) \quad (1)$$

$$\%M_{WB} = \left(\frac{W_w}{W_w + W_{dr}} \right) \times 100 \quad (2)$$

where W is the primary weight (g) of the product, W_w is the mass (g) of the water in the food, and W_{dr} is the mass (g) of the dry product [27].

The moisture ratio (MR) is related to moisture content as follows:

$$MR = \frac{M_t - M_e}{M_i - M_e} \quad (4)$$

where M_e [g water / (g dry matter)] is the equilibrium moisture content at the end of drying, and M_i [g water / (g dry matter)] is the initial moisture content.

2.2. Mathematical Modeling for the Numerical Analysis

The energy conservation equation in solids can be given as follows;

$$\rho c_p \left(\frac{\partial T}{\partial t} \right) + \nabla(-k\nabla T) = 0 \quad (5)$$

where c_p is specific heat of food [J/(kg K)], k is the thermal conductivity of food [W/(mK)], ρ is the density of food [kg/m³] and the mass conservation equation in solids can be given as follows [28]:

$$\frac{\partial M}{\partial t} + \nabla(-D_{eff}\nabla M) = 0 \quad (6)$$

where D_{eff} is the effective diffusion coefficient (m²/s) and M is the moisture content (g water/g material).

2.2.1. First and Boundary Conditions

The first moisture content of the carrot, eggplant, and cucumber was obtained to be 79.51%, 92.3%, and 88.56%, respectively and the initial temperature of the food was 15 °C.

2.2.2. Heat Transfer Boundary Conditions

The surface boundary condition for heat transfer is given below:

$$-n(-k\nabla T) = h_t(T - T_s) \quad (7)$$

where h_t is the heat transfer coefficient [W/(m²K)] and T_s is the drying air temperature (°C). The symmetry boundary condition for heat transfer is presented below:

$$n(k\nabla T) = 0 \quad (8)$$

2.2.3. Mass Transfer Boundary Conditions

The surface boundary condition for mass transfer is given below:

$$-n(D\nabla M) = h_m(M - M_s) \quad (9)$$

where h_m is the mass transfer coefficient (m/s), and M_s is the equilibrium moisture content (g water/g material). The symmetry boundary condition for mass transfer is presented below:

$$n(D\nabla M) = 0 \quad (10)$$

2.3. Heat and Mass Transfer Coefficients

Heat transfer coefficients can be calculated with well-known correlations in the literature [29].

$$Nu = \frac{h_T L}{k} = 0.664 Re^{0.5} Pr^{0.33} \quad (11)$$

$$Sh = \frac{h_M L}{D_{AB}} = 0.664 Re^{0.5} Sc^{0.33} \quad (12)$$

The Reynolds number ranges from 922.99 to 1292.19. Thus, the expression given in Eq. 11 and 12 is suitable since it is a laminar flow.

2.4. Data Analysis

Five different experimental, semi-experimental, and thin layer drying models (the Lewis model, Henderson and Pabis model, Two Term model, Wang and Singh model, and Midilli model) used in the literature were applied. (see Table 1)

Table 1. Constants and coefficients of the drying models

Model No	Name of Model	Model	Reference
1	Lewis	MR=exp(-kt)	[7]
2	Henderson and Pabis	MR=aexp(-kt)	[8]
3	Two Term	MR=aexp(-k ₀ t)+bexp(-k ₁ t)	[9]
4	Wang and Singh	MR=1+at+bt ²	[10]
5	Midilli	MR=aexp(-kt ⁿ)+bt	[11]

MR: moisture ratio, k, k₀, k₁: drying constant (min⁻¹), a, b: coefficient, n: drying constant

Statistical parameters were calculated using the Sigma Plot program. The drying coefficients (a, b, k, k₀, k₁, n) and the coefficients of determination (R²), standard error of estimate (SEE), and chi-square (x²) expressions, which are statistical parameters, were calculated as follows [30]:

$$SEE = \sqrt{\frac{\sum_{i=1}^N (MR_{exp} - MR_{pred})^2}{N-z}} \tag{13}$$

$$x^2 = \frac{\sum_{i=1}^N (MR_{exp} - MR_{pred})^2}{N-z} \tag{14}$$

where MR_{experimental} is experimental moisture ratio, MR_{predicted} is the predicted moisture ratio, N is the number of experimental data points, and z is the number of parameters in the model. It is difficult to figure out the shrinkage effect experimentally. The shrinkage rate at any point of the food is defined as follows:

$$u(x) = u(b) \frac{x}{b} \tag{15}$$

The shrinkage rate value on the surface is given in Eq. (15).

$$u(b) = \frac{b - b(old)}{\Delta t} \tag{16}$$

where, b (old) is the half-thickness of the food at the next time step, and b is the initial half-thickness [31]. In order to figure out the half-thickness of the food at any time, the following expression obtained depending on the moisture content of the food at that time is used.

$$b = b_0 \left[\frac{\rho_w + M \rho_s}{\rho_w + M_0 \rho_s} \right] \tag{17}$$

2.5. Uncertainty Analysis

It is necessary to determine the total error by performing the uncertainty analysis of the measurement results. The overall uncertainty can be estimated using the following expressions:

$$W_r = \left[\left(\frac{\partial R}{\partial x_1} w_1 \right)^2 + \left(\frac{\partial R}{\partial x_2} w_2 \right)^2 + \dots + \left(\frac{\partial R}{\partial x_n} w_n \right)^2 \right]^{\frac{1}{2}} \tag{18}$$

$$e = \frac{W_r}{R} \tag{19}$$

where, R (x₁, x₂, x₃, ... x_n) is a function of independent variables, W_r is the overall uncertainty, w₁, w₂, w₃, ... w_n are error values of the independent variables and e is the relative uncertainty [32]. Uncertainty analysis of moisture content was performed using Eqs. 18-19. The relative uncertainties for cucumber, eggplant, and carrot were obtained to be ± 0.5%, 0.7%, and 0.3%, respectively. Sensitivity values and total uncertainty values of the measuring devices are given in Table 2.

Table 2. Total uncertainty values of the measuring devices used in the drying test

Device	Parameter	Accuracy (\pm)	Uncertainty (\pm)	Overall uncertainty (\pm)
Dryer	Air temperature	0.3 °C	0.1	0.3162
	Air velocity	0.1 m/s	0.1	0.1414
Temperature sensor	Food temperature	0.5°C	0.1	0.5099
Digital scale	Food weight	0.05 g	0.01	0.0509

3. RESULTS AND DISCUSSION

3.1. Experimental Drying Kinetics

Figure 3 shows the drying behaviour of different foodstuffs under the same air velocity (0.7 m/s) and air temperature (60°C). As shown in Figure 3a, at the end of the 180 minute drying period, the moisture content of each foodstuff (cucumber, carrot, and eggplant) is obtained as 2.95 [g/g dry], 1.28 [g/g dry] and 2.01 [g/g dry], respectively. The change in moisture content of each foodstuff is calculated as 61%, 66%, and 83%. The surface temperatures are also shown in Figure 3b. The measured surface temperature values increased from 14.5°C to about 57°C. The surface temperature values for cucumber are higher than those for carrot and eggplant. The surface temperature values for cucumber, carrot, and eggplant are calculated to be 55.6°C, 52.5°C, and 47°C at the end of the 3 hour drying process. Since the moisture content in the product decreases throughout the drying process, the obtained data are also compatible with the conclusions of some studies in the literature [9, 31, 33, 34, 35].

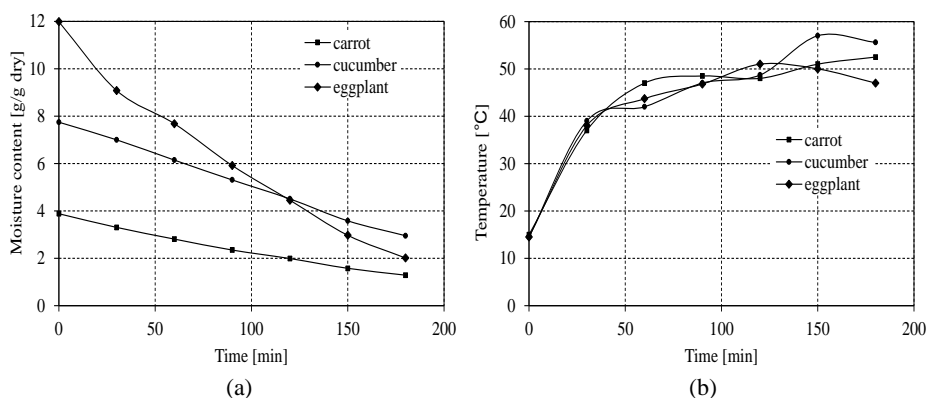


Figure 3. (a) Moisture content, (b) temperature versus drying time for different foodstuffs (carrot, cucumber and eggplant) at a drying temperature of 60°C and an air velocity of 0.7 m/s

The experimental data on moisture content obtained at a drying air temperature of 60°C for five well-known semi-empirical models are given in Table 1.

Table 3. Statistical parameter values and coefficients obtained for carrot, cucumber and eggplant

Model	Carrot Constants and coefficients			Cucumber Constants and coefficients			Eggplant Constants and coefficients		
	R ²	SEE	x ²	R ²	SEE	x ²	R ²	SEE	x ²
1	0.99	0.0149	0.0002	0.97	0.0345	0.0012	0.98	0.0320	0.0010
2	0.99	0.0148	0.0002	0.98	0.0321	0.0010	0.98	0.0347	0.0012
3	0.99	0.0191	0.0004	0.98	0.0415	0.0017	0.98	0.0448	0.0020
4	0.99	0.0054	2.95×10 ⁻⁵	0.99	0.0086	7.42×10 ⁻⁵	0.99	0.0230	0.0005
5	0.99	0.0061	3.71×10 ⁻⁵	0.99	0.0077	6.00×10 ⁻⁵	0.99	0.0169	0.0003
1	k=0.0058			k=0.0047			k=0.0086		
2	k=0.0059		a=1.0123	k=0.0050		a= 1.0345	k=0.0087		a=1.0099
3	a=0.47		b=0.85	a=0.49		b=0.53	a=0.49		b=0.51
	k ₀ =0.0059		k ₁ =0.0059	k ₀ =0.0050		k ₁ =0.0050	k ₀ =0.0087		k ₁ =0.0087
4	a=-0.005		b=7.23×10 ⁻⁶	a=-0.0035		b=5.88×10 ⁻⁸	a=-0.0069		b=1.26×10 ⁻⁵
5	a=0.99		b=-0.0007	a=0.99		b=-0.0008	a=0.99		b=-0.0025
	n=0.97		k=0.0049	n=1.22		k=0.0012	n=0.59		k=0.0224

R², the coefficient of determination; SEE, standard error of estimate; x², chi-square; k, k₀, k₁, drying constant (min⁻¹); a, b, coefficients; n, drying constant

The statistical results (a, b, k, k₀, k₁, n, R², SEE, and x²) obtained from these models' coefficients were presented collectively in Table 3. To describe the most appropriate model using the dimensionless moisture content obtained from the experiment, the R² value should be close to 1, and the SEE and x² values should be close to 0 [35]. In accordance with these results (Table 3), the largest R² and the smallest SEE and x² values for cucumber and eggplant were obtained in Midilli model. However, the best model for carrot was obtained in the Wang and Singh model. It is possible to say that the Midilli model gives better predictions among the other models and is the most appropriate model for cucumber and eggplant.

Using the SigmaPlot software, predicted moisture ratio values for the Midilli Model are calculated for each food. The verification of the Midilli model was assessed by equating the computed moisture ratio with the observed moisture ratio. The results for foodstuffs are shown in Figure 4. The regression coefficients (R²) for each foodstuff (carrot, cucumber, and eggplant) were obtained to be 0.9997, 0.9994, and 0.9984, respectively. A 45° straight line between the experimental and predicted ratios points out that the Midilli model is a good predictor. It is possible that the estimated data obtained for the experimental and Midilli model are close to each other in the direction of y = x (R² = 1). In order to achieve this equation, the values in the x and y axis must be on the 45° straight line.

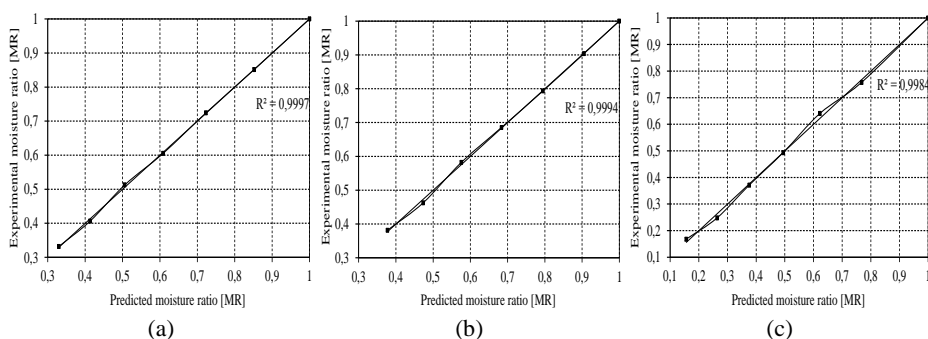


Figure 4. The correlation between the experimental moisture ratio and predicted moisture ratio for different foodstuffs (a-carrot, b-cucumber, c-eggplant)

3.2. Numerical Study and Verification

A two-dimensional axisymmetric model was used to describe the heat and mass transfer equations in the hot air convection dehydration process. Due to the axial symmetry of the food slabs, only a quarter of the planing intersection was taken into account in the numerical method. It is observed in the literature that this model approach has been preferred in some numerical drying studies [17, 31].

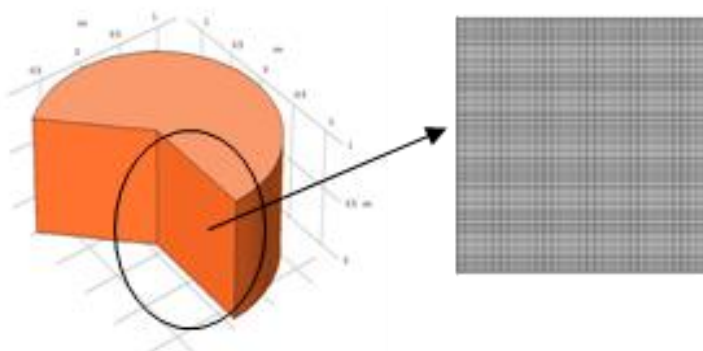


Figure 5. The model used in analyses and mesh structure

The assumptions made for the simulation are as follows;

- There is no heat production inside the food.
- The heat transfer in the food was take place by conduction (Fourier’s law), and mass transfer was considered to take place by diffusion (Fick’s law).
- The shrinkage effect was considered during the drying period.
- The thermophysical properties of the air and food were constant.
- The temperature and velocity of the drier air were constant.

Food materials were modelled for numerical simulation. Different mesh structures were applied to foods (Figure 5). The mesh independence study of moisture content was carried out, and the maximum difference was found to be 1%. What is important in mesh independence studies is that there is an acceptable difference (1%) between the results obtained for different mesh numbers. In addition, analysis time should be taken into consideration in determining the

number of mesh [36]. Finally, for the accurate solution, a grid structure consisting of 8000 quadrilateral elements, 360 edge elements, and 4 vertex elements was selected. The nonlinear PDEs (partial differential equations) were solved using Comsol Multiphysics 5.3 [37] with the relative tolerance of 0.001. The parameters and thermophysical properties used in the analyses are presented in Table 4. The deformed mesh was used to consider the volume change due to the fluid transfer. Therefore, the Arbitrary Lagrange Eulerian (ALE) method was applied in Comsol Multiphysics 5.3. The ALE method is used as an application between the Lagrangian and Eulerian approaches that allow the identification of moving boundaries. The Laplace smoothing type was defined as the deformed mesh. Figure 6 indicates the variation in the moisture content of carrot under the shrinkage effect with time. The increasing shrinkage effect was obtained during drying. Initially all foods has a radius of 1.25 cm and a thickness of 1 cm. After 1, 2, and 3 hours, the amount of decrease in the volume of the carrot was determined to be 22.8% (radius 1.15 cm, thickness 0.91 cm), 42% (radius 1.05 cm, thickness 0.82 cm), and 55.7% (radius 0.98 cm, thickness 0.72 cm). Similarly, the shrinkage effect in cucumber during drying is given in Figure 7. After 1, 2, and 3 hours, the percentage change in the product volume was calculated to be 21.6% (radius 1.16 cm, thickness 0.91 cm), 41% (radius 1.06 cm, thickness 0.82 cm), and 55.7% (radius 0.98 cm, thickness 0.72 cm).

Table 4. Thermophysical properties and experimental drying conditions of the carrot, cucumber, and eggplant

Parameter	Value	Reference
Air velocity (m/s)	0.7	
Food temperature (°C)	15	
Food density (kg/m ³)	1029-950-571	[38, 39, 40]
Air temperature (°C)	60	
Food moisture content (% w.b.)	79-88-92	
Air relative moisture (%)	79	
Thermal conductivity of food (W/mK)	0.569-0.62-0.356	[38, 39, 40]
Specific heat (J/kgK)	3849-4030-3900	[38, 39, 40]
Heat of vaporization (kJ/kg)	2466	
Water density (kg/m ³)	999.1	
Heat transfer coefficient (W/m ² K)	20.33	
Mass transfer coefficient (m/s)	0.0190	
Shrinkage velocity (m/s) × 10 ⁷	2.481-2.527-3.370	
Moisture diffusivity (m ² /s) × 10 ¹⁰	9.374-8-9.6883	[41, 42, 43]

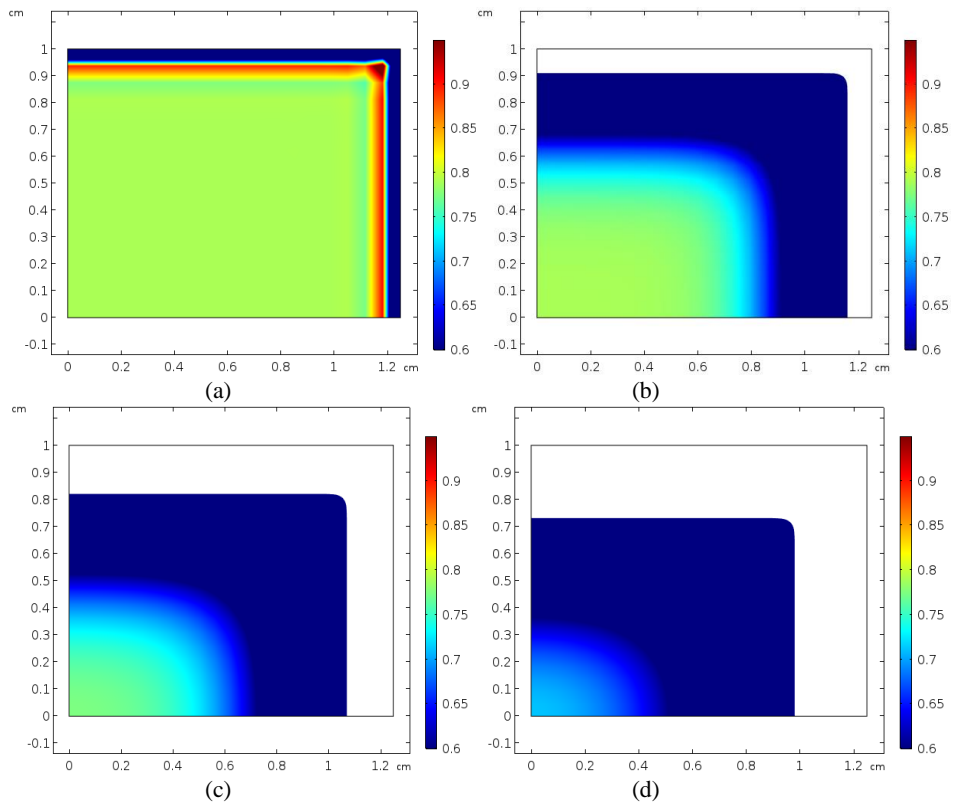


Figure 6. Evolution in the moisture content of the carrot over time during the drying process considering the shrinkage effect (a-Start of drying, b-1.h , c- 2.h, d- 3.h)

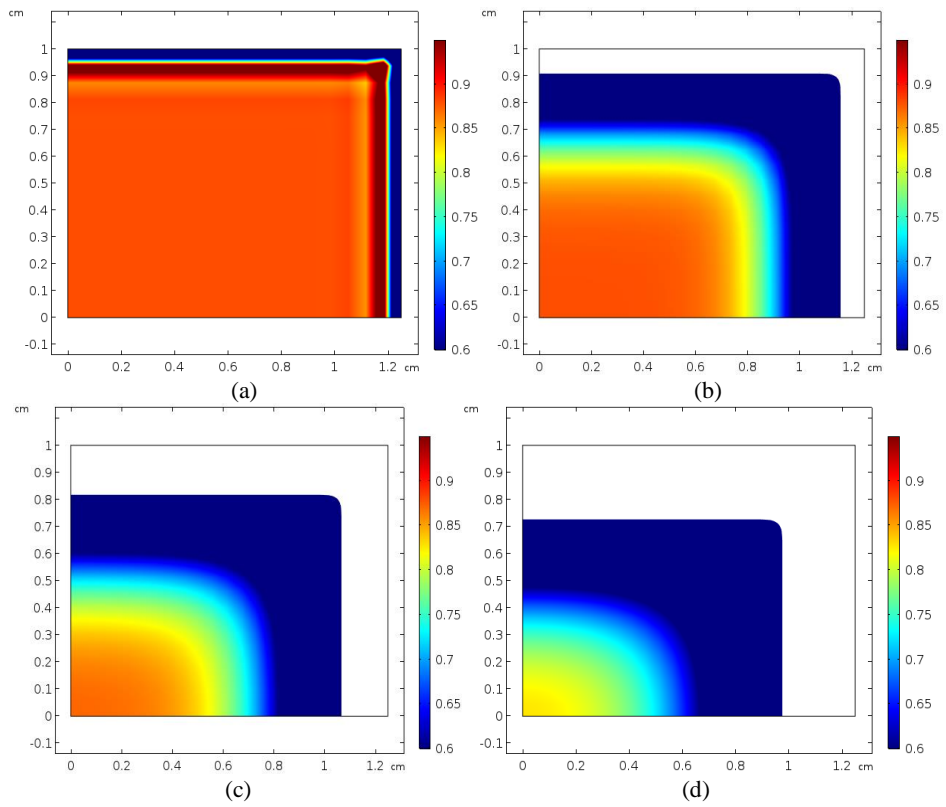


Figure 7. Evolution in the moisture content of the cucumber over time during the drying process considering the shrinkage effect (a-Start of drying, b-1.h , c- 2.h, d- 3.h)

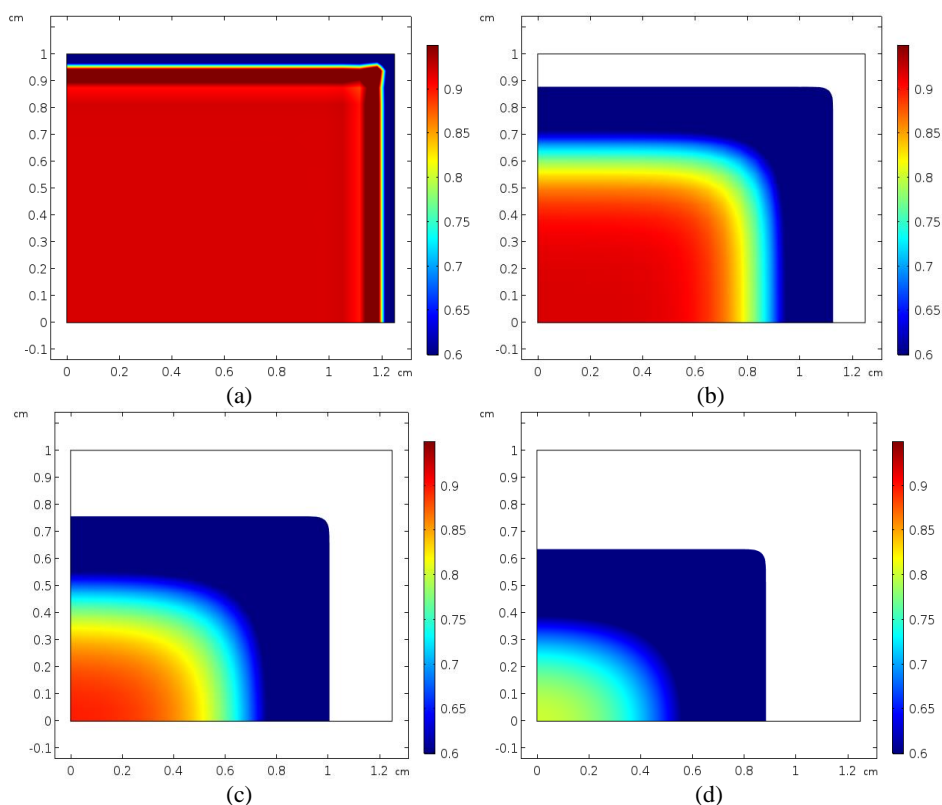


Figure 8. Evolution in the moisture content of the eggplant over time during the drying process considering the shrinkage effect (a-Start of drying, b-1.h , c- 2.h, d- 3.h)

The percentage change in the volume of eggplant was obtained to be 37.8% (radius 1.05 cm, thickness 0.88 cm), 51.4% (radius 1 cm, thickness 0.76 cm) and 68.7% (radius 0.88 cm, thickness 0.63 cm) respectively, at the end of the 1st, 2nd, and 3rd hours of drying. At the end of 3 hours, the volume of carrot and cucumber was $2.17 \times 10^{-6} \text{ m}^3$ while the volume of eggplant was calculated to be $1.53 \times 10^{-6} \text{ m}^3$. According to the results obtained from Figure 6, 7, 8, it can be said that the effect of shrinkage appeared most in the eggplant. The volume changes of carrot and cucumber are very close to each other. The numerical model was verified by comparing the moisture content and temperature values obtained from experiments. Figure 9 (a-b-c) indicates the changing of the moisture content values obtained from the experiments with the average moisture content values derived from the analysis of different foodstuffs. A difference of approximately 2.7%, 2.4%, and 0.8% was found between the values derived from the experiments and analyses for carrot, cucumber, and eggplant. The temperature values of the product center were experimentally measured and numerically calculated during drying. As a result, a very good fit between the numerical and experimental results was found. Since the moisture distribution inside food is variable, it is difficult to calculate moisture content experimentally. However, the moisture distribution in the food can be estimated by using simulation. The amount of evaporation from the food surface is higher when compared to the center. If the dry state cannot be provided, liquid remaining inside food causes to form microorganisms in the food [29]. Therefore, it is important

to accurately determine the moisture content distribution in the food and the drying time by simulation.

Drying is a complex, dynamic, non-linear process that simultaneously depends on many parameters. Therefore, the determination of drying processes is important for both academic and industrial users. In order to determine the optimum conditions in drying processes, the test process is costly and time consuming. Therefore, simulations are performed to reduce time and reduce costs. In this way, optimum drying conditions can be determined. In this study, the experimental study is also modeled numerically and results are found to be close to each other. Furthermore, the storage and transportation of dried foods are important in terms of cost. Therefore, the volume changes of the products should also be considered. Determination of volume change can be done numerically as seen in this study.

In experimental processes, the average moisture content of the product is calculated by measuring weight changes. However, the moisture content distribution in the product is not equal. Simulations provide us with a numerical solution to detect this situation. Thus, after drying, it can be determined which parts of the product have a high amount of moisture, and this knowledge will allow for a more efficient and healthier drying process.

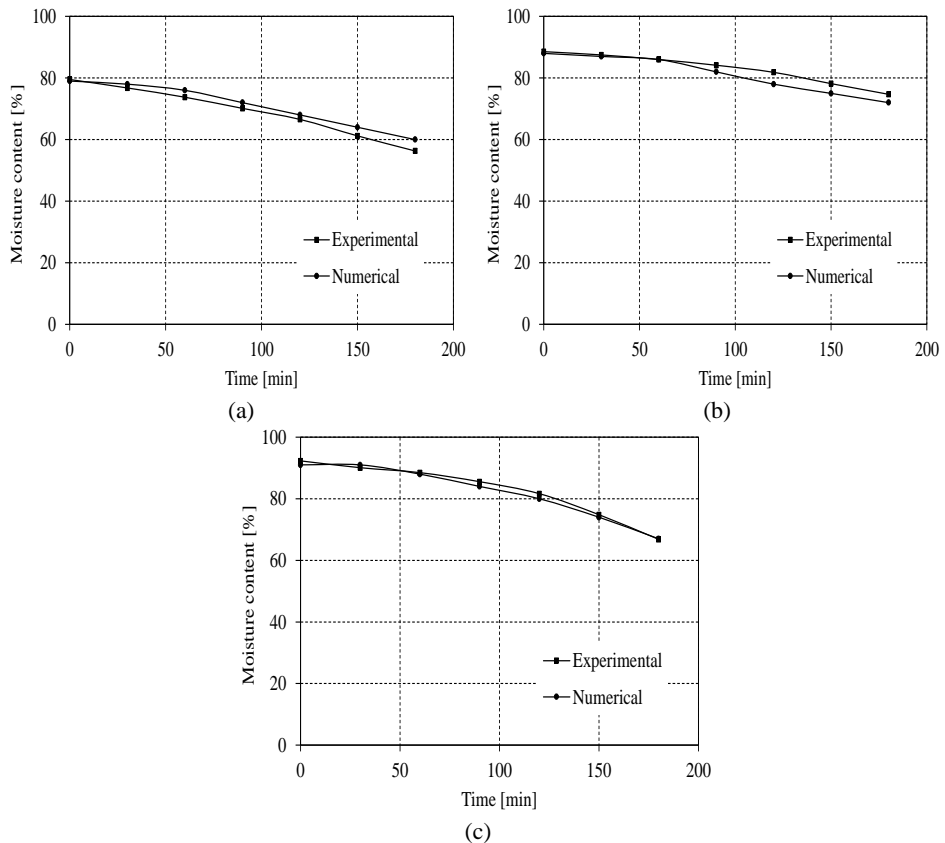


Figure 9. Variation numerical model with shrinkage and experimental study (a- carrot, b- cucumber, c-eggplant)

4. CONCLUSION

In this study, the dehydration kinetics of carrot, cucumber and eggplant were studied experimentally. Five different thin film drying models have been used in the literature to find the optimal model for the data from the experiment. Models considering the shrinkage effect were developed in order to define the drying characteristics. The volumetric shrinkage rates of food products were examined. Finally, the numerical results were matched with the empirical results. The numerical results were found to be in considerable compromise with the empirical results. The results can be summarized as follows:

As a result of the nonlinear regression analysis, it can be said that the best model for defining the drying kinetics of cucumber, and eggplant is the Midilli model. However, Wang and Singh model is the best model for carrot.

According to the obtained results, at the air temperature of 60°C and air velocity of 0.7 [m/s], the fastest drying was determined in the eggplant. Therefore, eggplant should be preferred to carry out a faster-drying process.

The shrinkage effect was calculated for the change in the product volume, and the maximum volumetric change was realized for eggplant with 68.7%.

The moisture values obtained from the experimental study were compared with numerical analysis and found to be compatible. According to the results, the mathematical model (including the shrinkage effect) expressing simultaneous heat and mass transfer can be used to estimate the moisture and temperature distribution in the product during drying. Thus, it is possible to discuss how drying can be done in advance. The aim is to obtain a homogeneous moisture distribution throughout the product after drying. In this way, better quality products can be obtained by preventing the deterioration of the product.

Nomenclature

c_p	specific heat (kJ/kgK)
D_{eff}	effective moisture diffusivity (m^2/s)
D_0	coefficient
h_m	mass transfer coefficient (m/s)
h_t	heat transfer coefficient ($\text{W}/\text{m}^2\text{K}$)
k	thermal conductivity of food (W/mK)
L	length (m)
MR	moisture ratio
N	number of experimental data points
Nu	Nusselt number = $h_T L/k$
Pr	Prandtl number = ν/α
Re	Reynolds number = uL/ν
R^2	coefficient of determination
S_b	shrinkage coefficient (%)
Sc	Schmidt number = ν/D_{AB}
Sh	Sherwood number = $h_m L/D_{AB}$
SEE	standard error of estimate
t	drying time (min)
T	temperature (K)
u	air velocity (m/s)
V	volume (m^3)
χ^2	chi-square
ρ	density (kg/m^3)
ν	viscosity (m^2/s)

Subscripts

b, oinitial, reference
e equilibrium
h air
DB dry basis
s solid, surface
t time, moment
w water
WB wet basis

REFERENCES

- [1] Singh B., Gupta A.K., (2007) Mass transfer kinetics and determination of effective diffusivity during convective dehydration of pre-osmosed carrot cubes, *Journal of Food Engineering*, 79, 459-470.
- [2] Lima K. S., Cople A.L.S., Lima L.C., Freitas R.C., Della-Modesta R.L., Godoy O., (2004) Effect of Low Doses of Irradiation on the Carotenoids in Ready-to-Eat Carrots, *Food Science and Technology (Campinas)*, 24(2), 183–193.
- [3] Puig A., Perez-Munuera I., Carcel J.A., Hernando I., Garcia-Perez J.V., (2012) Moisture loss kinetics and microstructural changes in eggplant (*Solanum melongena* L.) during conventional and ultrasonically assisted convective drying, *Food and Bioprocess Technology*, 90, 624–632.
- [4] Alibas I., (2006) Characteristics of chard leaves during microwave, convective, and combined microwaveconvective drying, *Drying Technology*, 24(1), 1425-1435.
- [5] Lima A.G.B., Queiroz M.R., Nebra S.A., (2002) Simultaneous moisture transport and shrinkage during drying solids with ellipsoidal configuration, *Chemical Engineering Journal*, 86, 83–85.
- [6] Avcı A., Can M., (1999) The analysis of the drying process on unsteady forced convection in thin films of ink, *Applied Thermal Engineering*, 19, 641-657.
- [7] Lewis W. K., (1921) The rate of drying of solid materials, *J. Ind. Eng. Chem.*, 13(5), 427–432.
- [8] Henderson S. M., Pabis S., (1961) Grain drying theory I: temperature effect on drying coefficient, *J. Agr. Eng. Resource*, 6(3), 169–174.
- [9] Madamba P. S., Driscoll R. H., Buckle K. A., (1996) The thin layer drying characteristics of garlic slices, *Journal of Food Engineering*, 29(1), 75-97.
- [10] Wang C. Y., Singh R. P., (1978) A single layer drying equation for rough rice, *ASAE*, Paper No: 78-3001, St. Joseph, MI.
- [11] Midilli A., Kucuk H., Yapar Z., (2002) A new model for single layer drying, *Drying Technology*, 20(7), 1503-1513.
- [12] Vega A. M. N., Sturm B., Hofacker W., (2016) Simulation of the convective drying process with automatic control of surface temperature, *Journal of Food Engineering*, 170, 16-23.
- [13] Bezerra C.V., Silva L.H.M., Corrêa D. F., Rodrigues A.M.C., (2015) A modeling study for moisture diffusivities and moisture transfer coefficients in drying of passion fruit peel, *International Journal of Heat and Mass Transfer*, 85, 750–755.
- [14] Udayraj Md. A., Mishra R. K., Chandramohan V.P., Talukdar P., (2014) Numerical modeling of convective drying of food with spatially dependent transfer coefficient in a turbulent flow field, *International Journal of Thermal Sciences*, 78, 145-157.
- [15] Kaya A., Aydın O., Kamer M. S., Doğan O., (2013) Su Kabağının Kuruma Davranışının Deneysel İncelenmesi, *KSÜ Mühendislik Bilimleri Dergisi*, 16(2).

- [16] Lemus-Mondaca R. A., Zambra C.E., Vega-Gálvez A., Moraga N.O., (2013) Coupled 3D heat and mass transfer model for numerical analysis of drying process in papaya slices, *Journal of Food Engineering*, 116, 109–117.
- [17] Kumar C., Karim A., Koardder M.U.H., Miller G.J., (2012) Modeling Heat and Mass Transfer Process During Convection Drying of Fruit, *4th International Conference on Computational Methods (ICCM 2012)*, Australia.
- [18] Darıcı S., Şen S., (2012) Kivi Meyvesinin Kurutulmasında Kurutma Havası Hızının Kurumaya Etkisinin İncelenmesi, *Tesisat Mühendisliği*, 130.
- [19] Doymaz I., (2005) Drying characteristics and kinetics of okra, *Journal of Food Engineering*, 69: 275 – 279.
- [20] Sabarez H. T., (2012) Computational modelling of the transport phenomena occurring during convective drying of prunes, *Journal of Food Engineering*, 111: (2) 279–288.
- [21] Simal S., Garau C., Femenia A., Rossello C., (2005) Drying of red pepper (*Capsicum annum*): water desorption and quality, *International Journal of Food Engineering*, 1:(4), 1-14.
- [22] Doymaz I., (2017) Drying kinetics, rehydration and colour characteristics of convective hot-air drying of carrot slices, *Heat and Mass Transfer*, 53, 25-35.
- [23] Zhu A., Shen X., (2014) The model and mass transfer characteristics of convection drying of peach slices, *Int J Heat and Mass Trans.*, 72: 345-351.
- [24] Taheri-Garavand A., Rafiee A., Keyhani A., (2011) Mathematical Modeling of Thin Layer Drying Kinetics of Tomato Influence of Air Dryer Conditions. *Int. Trans. J Eng. Manag& Applied Sci&Technol.* 2: 147-160.
- [25] Maskan M., 2001, Drying, shrinkage and rehydration characteristics of kiwi fruits during hot air and microwave drying. *Journal of Food Engineering* 48: 177–182.
- [26] Zlatanovic I., Komatina M. and Antonijevi D., 2013, Low-temperature convective drying of apple cubes. *Applied Thermal Engineering* 53:114-123.
- [27] Doymaz I., Tugrul N., Pala M., (2006) Drying characteristics of dill and parsley leaves, *Journal of Food Engineering*, 77, 559-565.
- [28] Sabarez H. T., (2012) Computational modelling of the transport phenomena occurring during convective drying of prunes, *Journal of Food Engineering*, 111(2), 279–288.
- [29] Kumar C., Millar G. J., Karim M. A., (2015) Effective diffusivity and evaporative cooling in convective drying of food material, *Drying Technology*, 33, 227-237.
- [30] Goyal R. K., Kingsly A. R. P., Mainkanthan M. R., Ilyas S. M., (2007) Mathematical modeling of thin-layer drying kinetics of plum in a tunnel dryer, *Journal of Food Engineering*, 79(1), 176-180.
- [31] Karim M. A., Hawlader M. N. A., (2005) Mathematical modelling and experimental investigation of tropical fruits drying, *International Journal of Heat and Mass Transfer*, 48(23), 4914-4925.
- [32] Moffat R.J., (1988) Describing the uncertainties in experimental results, *Experimental Thermal and Fluid Science*, 1(1), 3-17.
- [33] Turkan B., Etemoglu A.B., Can M., (2019) An Investigation Into Evaporative Ink Drying Process on Forced Convective Heat and Mass Transfer Under Impinging Air Jets, *Heat and Mass Transfer*, 55(5), 1359-1369.
- [34] Turkan B., Etemoglu A.B., (2019) Numerical investigation of wood drying, *Wood Research*, 64(1):127-136.
- [35] Pangavhane D. R., Sawhney P. N., Sarsavadia P. N., (1999) Effect of various dipping pretreatments on drying kinetics of thompson seedless grapes, *Journal of Food Engineering*, 39, 211-216.
- [36] Chilka A. G., Ranade, V. V., (2017) Drying of Almonds I: Single Particle, *Indian Chemical Engineer*, 60:3, 232-254.

- [37] Comsol Multiphysics 5.3., (2019) Heat Transfer Model Library, *Heat Transfer Module User's Guide*, Chemical Reaction Engineering Module User's Guide.
- [38] Adams C., (1975) Nutritive Value of American Foods, Agriculture Handbook, No. 456, *Agricultural Research Service*, U.S. Department of Agriculture, Washington, DC.
- [39] Fasina O.O., Fleming H.P., (2001) Heat transfer characteristics of cucumbers during blanching, *Journal of Food Engineering*, 47, 203–10.
- [40] Ali S. D., Ramaswamy H. S., Awuah G. B., (2002) Thermo-Physical Properties of Selected Vegetables as Influenced by Temperature and Moisture Content, *Journal of Food Process Engineering*, 25, 417-433.
- [41] Togrul H., (2006) Suitable drying model for infrared drying of carrot, *Journal of Food Engineering*, 77, 610–619.
- [42] Shahari N., Hussein S.M., Nursabrina M., Hibberd S., (2014) Mathematical modelling of cucumber (*cucumis sativus*) drying, *Proceedings of the 21st National Symposium on Mathematical Sciences (SKSM21) AIP Conf. Proc.* 1605, 307-312.
- [43] Guine R. P. F., Brito M. F. S., Ribeiro J. R. P., (2017) Evaluation of Mass Transfer Properties in Convective Drying of Kiwi and Eggplant, *International Journal of Food Engineering*, 13(7), 13 pp.